

# TAMING THE TRI-SPACE TENSION: ARC-GUIDED HALLUCINATION MODELING AND CONTROL FOR TEXT-TO-IMAGE GENERATION

Jianjiang Yang\*

University of Bristol

edisonyang109@gmail.com

Ziyan Huang†

South China University of Technology

bonnie.ziyan.huang@gmail.com

## ABSTRACT

Despite remarkable progress in image quality and prompt fidelity, text-to-image (T2I) diffusion models continue to exhibit persistent **"hallucinations"**, where generated content subtly or significantly diverges from the intended prompt semantics. While often regarded as unpredictable artifacts, we argue that these failures reflect deeper, structured misalignments within the generative process. In this work, we propose a cognitively inspired perspective that reinterprets hallucinations as trajectory drift within a latent alignment space. Empirical observations reveal that generation unfolds within a multiaxial cognitive tension field, where the model must continuously negotiate competing demands across three key critical axes: semantic coherence, structural alignment, and knowledge grounding. We then formalize this three-axis space as the **Hallucination Tri-Space** and introduce the **Alignment Risk Code (ARC)**: a dynamic vector representation that quantifies real-time alignment tension during generation. The magnitude of ARC captures overall misalignment, its direction identifies the dominant failure axis, and its imbalance reflects tension asymmetry. Based on this formulation, we develop the **TensionModulator (TM-ARC)**: a lightweight controller that operates entirely in latent space. TM-ARC monitors ARC signals and applies targeted, axis-specific interventions during the sampling process. Extensive experiments on standard T2I benchmarks demonstrate that our approach significantly reduces hallucination without compromising image quality or diversity. This framework offers a unified and interpretable approach for understanding and mitigating generative failures in diffusion-based T2I systems.

## 1 INTRODUCTION

*"Why do diffusion models sometimes turn "puppies" into "cats" or replace "blankets" with "carpets"? Why do such phenomena persist even for simple prompts? Can we understand, model, and control them?" (Figure. 1)*

Despite remarkable progress in image fidelity and prompt relevance, state-of-the-art text-to-image (T2I) diffusion models still exhibit persistent failures referred to as hallucinations, where generated images deviate from prompt intent. These errors are not mere artifacts. As illustrated in Figure. 1, even simple and unambiguous prompts can yield unexpected results like semantic substitutions (*e.g., turning a "puppy" into a "cat"*) or contextual mismatches (*e.g., replacing a "blanket" with a "carpet"*). Recent works have attributed such misalignments primarily to data noise and imbalanced attention during inference. For example, Chang et al. identify "catastrophic neglect" of prompt-specified objects in diffusion models and mitigate it via attention-guided enhancement Chang et al. (2024); Zhang et al. similarly improve prompt-image alignment by adjusting energy-based attention maps Zhang et al. (2024); Meanwhile, Lim and Shim propose retrieval-augmented generation to ground image factuality Lim & Shim (2024). While these approaches address hallucinations by refining attention or grounding mechanisms, they often treat failures as post-hoc fixes rather than

\*Equal contribution, first author.

†Equal contribution, second author.

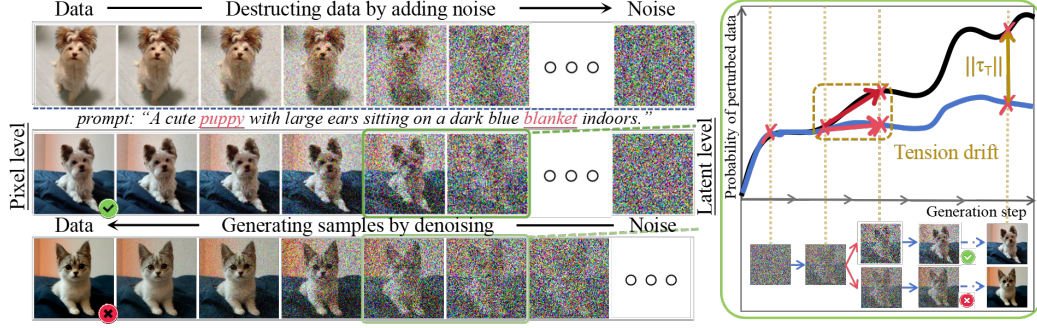


Figure 1: Visualizing hallucination as trajectory drift in latent alignment space. Successful generations (middle row) follow a coherent sampling trajectory from noise to data, remaining close to the prompt intent. Hallucinatory generations (bottom row) exhibit tension drift, leading to semantic and structural deviations.

emerging from fundamental misregulation of the generation process itself, overlooking the underlying dynamics of why and how the hallucination emerge.

We begin by revisiting a foundational question in the generative process of diffusion models: *Are hallucinations merely stochastic artifacts of sampling, or do they reflect deeper structural failures rooted in internal tension dynamics?* To eliminate ambiguity and isolate the source of failure, we construct a synthetic dataset in which each text prompt deterministically maps to a unique image (see Sec. 1.1). Surprisingly, even under these nearly ideal conditions, diffusion models consistently produce significant misalignments, ranging from shape swaps and color inversions to positional inconsistencies. Crucially, these failures are not random. Unsupervised clustering of hallucinated outputs reveals a remarkably stable structure: across diverse prompts and generations, errors consistently segregate into three well-separated categories: semantic drift, structural distortion, and factual misrepresentation. What initially appears as scattered output anomalies now unveils an intrinsic structure of failure modes, hinting at latent alignment axes embedded in the generation process.

A closer examination reveals that these hallucination types correspond to three fundamental cognitive trade-offs the model must continually negotiate: (1) Semantic Coherence: maintaining identity fidelity (e.g., generating a “puppy” rather than a “cat”); (2) Structural Alignment: preserving spatial and compositional correctness (e.g., avoiding positional swaps or shape mismatches); (3) Knowledge Grounding: ensuring factual and commonsense plausibility (e.g., distinguishing a “blanket” from a “carpet”). These findings challenge the traditional view of hallucinations as local attention failures or sampling noise. Instead, we argue they are symptomatic of a deeper phenomenon: the emergence of directional cognitive tension within the generative trajectory.

From this insight, we arrive at a pivotal conceptual shift: Text-to-image generation is not a static mapping but a dynamic traversal through a latent tension space. Each prompt implicitly defines a multiaxial cognitive tension field, and the diffusion process must iteratively traverse this space while balancing competing alignment forces. This dynamic process, termed **cognitive alignment tension**, unfolds throughout the denoising trajectory. When one or more tension axes dominate, they destabilize the generative equilibrium, causing the trajectory to drift off course. We denote this directional deviation as a **trajectory drift**  $\Delta \vec{t}$ , which manifests as a hallucination in the output. Ideally, the generation should evolve within a well-balanced region of latent space, or the ideal alignment manifold  $\mathcal{M}_{\text{ideal}}$ . However, the imbalance in alignment tensions disrupt this path, pulling the model away from intended semantics.

This realization leads us to a formal abstraction. Despite the seemingly diverse nature of hallucinations, their root causes consistently converge along three principal axes of alignment imbalance. We thus introduce the: **Hallucination Tri-Space**  $\mathcal{T}^3$ , a structured latent space spanned by three orthogonal tension axes: (1) Semantic Coherence (SC): the alignment between prompt entities and generated object categories; (2) Structural Alignment (SA): the fidelity of spatial layout and positional relationships; (3) Knowledge Grounding (KG): the factual and commonsense plausibility of generated content. Rather than merely classifying hallucinations,  $\mathcal{T}^3$  enables explicit modeling

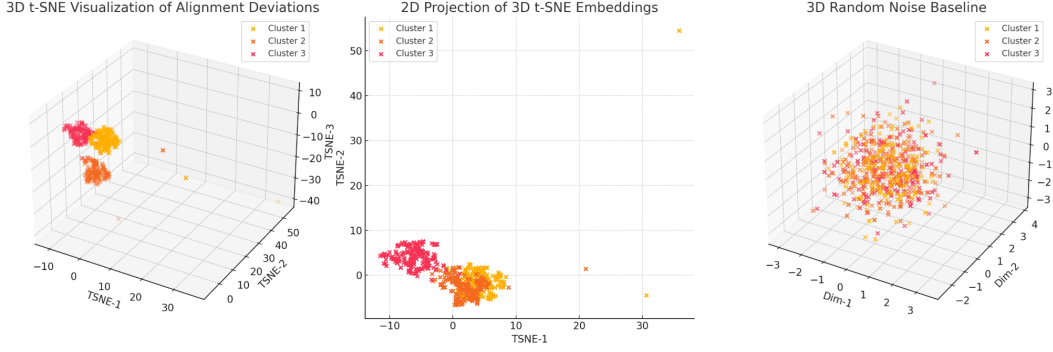


Figure 2: Unsupervised clustering of alignment deviation vectors in the Hallucination Tri-Space. **(a)** 3D t-SNE embedding of SC/SA/KG drift magnitudes shows three discernible clusters with realistic overlap, each corresponding to one dominant misalignment axis. **(b)** 2D projection of the same 3D embedding preserves the overall cluster structure despite mild inter-cluster mixing. **(c)** A truly random noise baseline yields no meaningful grouping, confirming that the observed clustering arises from structured alignment tensions rather than chance.

of tension dynamics. By tracking the directional shift  $\Delta \vec{t}$  within this space, we can quantitatively monitor tension imbalance during generation, offering a principled basis for real-time hallucination diagnosis and control.

To quantify the cognitive alignment tension, we project the trajectory drift  $\Delta \vec{t}$  onto the three axes of the Hallucination Tri-Space, yielding a real-time vector we term the **Alignment Risk Code (ARC)**:  $\vec{\tau}(p, t) = [\tau_{SC}(p, t), \tau_{SA}(p, t), \tau_{KG}(p, t)]^\top$ . This ARC vector models the live state of alignment tensions during sampling. Its magnitude reflects the overall cognitive stress, its imbalance indicates the degree of tension asymmetry, and its direction characterizes the dominant source of misalignment. Rather than diagnosing hallucinations after generation, ARC enables in-process monitoring of when and how generative deviation begins to emerge. To leverage this signal for intervention, we introduce the **TensionModulator (TM-ARC)**, a lightweight controller that operates fully within the latent space. TM-ARC interprets ARC dynamics and injects targeted, axis-specific corrections through three specialized submodules: (1) SC-Gate: mitigates semantic drift; (2) SA-Tuner: restores spatial integrity; (3) KG-Augment: reinforces factual grounding. Each submodule is activated with adaptive weights derived from the ARC vector, enabling fine-grained, real-time adjustment of the generative trajectory. This ensures the model remains within the ideal alignment manifold  $\mathcal{M}_{ideal}$  throughout the denoising process, significantly reducing hallucinations without compromising image diversity or quality.

We now look back at the three questions raised at the beginning: *Why do diffusion models sometimes turn "puppies" into "cats"? Why do such phenomena persist even for simple prompts? Can we understand, model, and control them?* **Our answer is:** hallucinations emerge when the generative trajectory is pulled off-course due to accumulating misalignments in semantic, structural, or factual dimensions during the sampling process. Specifically, "puppies" may become "cats" because of their close semantic similarity, and the model's failure to anchor fine-grained meanings. "Blankets" may be replaced by "carpets" when commonsense priors are weak and the model defaults to visually plausible substitutes. Even with simple prompts, these errors persist because the diffusion process is inherently a dynamic tension-balancing trajectory rather than a static semantic mapping. The persistence of hallucinations stems not from prompt complexity but from the accumulation of misalignments across multiple cognitive axes. We model this phenomenon using the ARC vector, which captures rising tensions in dimensions such as knowledge grounding and semantic coherence. Leveraging this signal, our TM-ARC controller actively intervenes during generation, steering the trajectory back toward the ideal manifold  $\mathcal{M}_{ideal}$ . Our contributions are threefold:

- We present the **Hallucination Tri-Space**  $\mathcal{T}^3$ , attributing hallucinations to systematic misalignments along three principal axes: semantic coherence (SC), structural alignment (SA), and knowledge grounding (KG).

Table 1: Clustering quality comparison across different feature spaces. Silhouette (higher is better) measures intra-cluster compactness vs inter-cluster separation; Calinski-Harabasz (higher is better) evaluates cluster dispersion; Davies-Bouldin (lower is better) penalizes overlapping clusters. Our alignment feature representation yields consistently superior clustering quality across all metrics.

Method	Silhouette $\uparrow$	Calinski-Harabasz $\uparrow$	Davies-Bouldin $\downarrow$
PCA	0.41	752.3	1.37
Random 3D Mapping	0.21	389.1	2.10
Alignment Features (Ours)	<b>0.63</b>	<b>1480.5</b>	<b>0.84</b>

- We formulate the **Alignment Risk Code (ARC)** vector, a real-time modeling of the three alignment tensions, capturing tension magnitude, imbalance, and skew and enabling fine-grained monitoring of generative deviation.
- We propose the **TensionModulator (TM-ARC)**, a lightweight controller that dynamically interprets ARC signals to inject targeted corrections during sampling, effectively steering the generation back toward  $\mathcal{M}_{\text{ideal}}$ .

### 1.1 EMPIRICAL CHARACTERIZATION OF HALLUCINATION PATTERNS IN ALIGNMENT TENSION SPACE

Before formalizing our framework in the following sections, we first present an empirical study to examine whether hallucinations in T2I models exhibit structured internal patterns. To isolate the generative mechanism from data or language ambiguity, we construct a controlled synthetic dataset with fully deterministic prompt-image mappings.

**Synthetic Setup.** We construct a synthetic dataset of 1000 prompt-image pairs, where each prompt unambiguously describes two geometric objects with specific shapes, colors, and spatial positions (*e.g.*, “A red circle on the left, and a green triangle on the right.”). We train a standard unconditional Denoising Diffusion Probabilistic Model (DDPM) on this dataset using fully unsupervised objectives, removing any external semantic signal or supervision.

**Observed Imbalance Patterns.** Despite the simplicity of the dataset, 27.8% of generated samples exhibit misalignments that violate prompt specifications. These include shape swaps, incorrect colors, and spatial reversals. Crucially, each error type can be mapped to one or more cognitive alignment axes (*e.g.*, *color errors*  $\rightarrow$  SC, *position flips*  $\rightarrow$  SA, *shape errors*  $\rightarrow$  KG).

**Alignment Tension Space Characterization.** To further analyze this structured misalignment, we extract a 3-dimensional alignment deviation vector for each generated sample, reflecting its SC, SA, and KG drift magnitudes. Using unsupervised clustering on these vectors, we find that hallucinated samples form three well-separated clusters. As shown in Table 1, our alignment-based clustering significantly outperforms PCA and random projection baselines across multiple metrics. Figure 2 further visualizes this structured clustering in the hallucination tri-space  $\mathcal{T}^3$ .

## 2 RELATED WORK

**Text-to-Image Diffusion Models** Recent advances in text-to-image (T2I) diffusion models have significantly improved image synthesis quality and compositional controllability. Foundational models such as Stable Diffusion and its variants rely on iterative denoising guided by conditioning inputs, yet faithfully aligning multiple modalities remains a central challenge Wang et al. (2023); Wu et al. (2024). Existing models often struggle when handling complex prompts involving object relations, attributes, or scene layouts. Recent innovations such as SoftREPA Lee et al. (2025), VLAD Johnson & Wilson (2025), and ELBO-T2IAlign Zhou et al. (2025) propose more explicit alignment mechanisms. These include contrastive loss for semantic preservation, hierarchical prompt parsing, and ELBO-based calibration to address subtle alignment errors.

**Text-to-Image Diffusion Models** Recent advances in text-to-image (T2I) diffusion models have significantly improved image synthesis quality and compositional controllability. Foundational models such as Stable Diffusion and its variants rely on iterative denoising guided by conditioning inputs, yet faithfully aligning multiple modalities remains a central challenge Wang et al. (2023); Wu et al. (2024). Existing models often struggle when handling complex prompts involving object relations, attributes, or scene layouts. Recent innovations such as SoftREPA Lee et al. (2025), VLAD Johnson & Wilson (2025), and ELBO-T2IAlign Zhou et al. (2025) propose more explicit alignment mechanisms. These include contrastive loss for semantic preservation, hierarchical prompt parsing, and ELBO-based calibration to address subtle alignment errors.

**Alignment Control and Conditioning Misalignment** Recent methods attempt to improve condition adherence through attention modulation or conditioning decoupling. For example, Text-Anchored Score Composition (TASC) Wang et al. (2023) explicitly decomposes conditional scores to mitigate attention conflicts, while attention modulation frameworks dynamically adjust cross-attention maps to strengthen alignment fidelity Wu et al. (2024). Although these approaches improve adherence to individual conditions, they do not model holistic hallucination risks across semantic, structural, and knowledge dimensions. To tackle this, alignment-centric frameworks such as CoMat Jiang et al. (2024) and MCCD Li et al. (2025) integrate cross-modal consistency and collaborative scene parsing directly into the generation process. These approaches proactively model alignment gaps, offering more robust compositional generalization during generation rather than relying on post-hoc correction Lu et al. (2025); Lv et al. (2025).

**Hallucination Mitigation in Multimodal Generative Models** Hallucination has also been widely studied in large language models (LLMs) and multimodal LLMs. Recent efforts address hallucination detection Chen et al. (2024) and propose retrieval augmentation or consistency supervision for factual grounding Lv et al. (2025); Lu et al. (2025). However, most existing methods operate post-hoc, lacking proactive hallucination prevention during generation. In contrast, our work directly integrates alignment risk modeling into the T2I generation process.

### 3 DEFINITIONS AND PRELIMINARIES

We briefly review the T2I diffusion framework that forms the basis of our alignment tension modeling.

**Diffusion Process** Given a clean image  $x_0 \sim q(x)$  from the data distribution, the forward diffusion process adds Gaussian noise over  $T$  timesteps:

$$q(x_t | x_{t-1}) = \mathcal{N}(x_t; \sqrt{1 - \beta_t}x_{t-1}, \beta_t \mathbf{I}) \quad (1)$$

where  $\beta_t \in (0, 1)$  controls the noise level at step  $t$ . This process allows direct sampling from  $x_t$  via:

$$q(x_t | x_0) = \mathcal{N}(x_t; \sqrt{\bar{\alpha}_t}x_0, (1 - \bar{\alpha}_t)\mathbf{I}) \quad (2)$$

with  $\bar{\alpha}_t = \prod_{j=1}^t (1 - \beta_j)$ .

The reverse process learns to denoise through a parameterized model  $p_\theta$ :

$$p_\theta(x_{t-1} | x_t) = \mathcal{N}(x_{t-1}; \mu_\theta(x_t, t), \Sigma_\theta(x_t, t)) \quad (3)$$

where  $\mu_\theta$  is typically computed from predicted noise  $\epsilon_\theta(x_t, t)$ .

In T2I diffusion, generation is conditioned on text embeddings  $c$ , modifying the denoising objective to predict  $p_\theta(x_{t-1} | x_t, c)$ .

### 4 WHY DO T2I DIFFUSION MODELS HALLUCINATE?

While prior studies have largely attributed hallucinations in text-to-image (T2I) diffusion models to data artifacts, sampling noise, or attention imprecision, we propose a more fundamental explanation: hallucinations reflect systematic misregulation of multi-axial cognitive tensions during the generative process. Rather than treating hallucinations as isolated, stochastic anomalies, we interpret them as

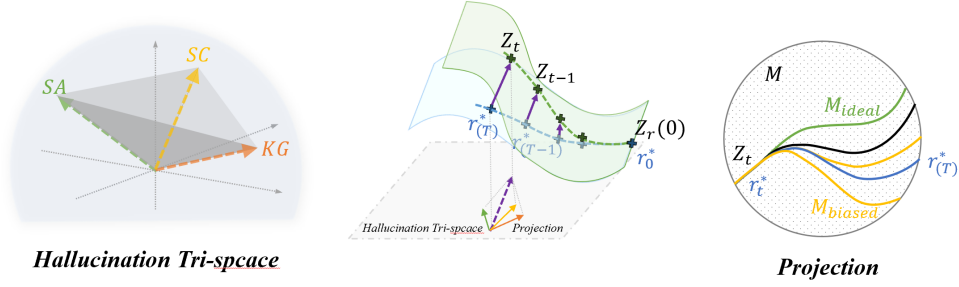


Figure 3: The figure illustrates how imbalanced semantic, structural, and knowledge tensions drive trajectory drift in T2I generation. The Alignment Risk Code (ARC) captures real-time multiaxial tension, enabling interpretable modeling and dynamic hallucination mitigation.

structured deviations arising from an imbalance among three core alignment objectives: *semantic coherence* (SC), *structural alignment* (SA), and *knowledge grounding* (KG). Each of these axes imposes directional constraints on generation and jointly defines a multiaxial tension space that the model must dynamically balance throughout the sampling trajectory.

#### 4.1 ALIGNMENT TENSION IMBALANCE.

Text-to-image (T2I) diffusion models synthesize images by progressively denoising latent representations conditioned on text prompts. Throughout this iterative process, the model must simultaneously satisfy three core alignment objectives: conveying prompt semantics (SC), maintaining spatial plausibility (SA), and ensuring factual correctness (KG). Each of these objectives imposes directional alignment pressure on the generative trajectory, collectively forming the Hallucination Tri-Space  $\mathcal{T}^3$ .

To model alignment dynamics within this space, we define a real-time cognitive tension vector:

$$\vec{\tau}(p, t) = [\tau_{SC}(p, t), \tau_{SA}(p, t), \tau_{KG}(p, t)]^\top \quad (4)$$

which captures the evolving alignment demands along each cognitive axis at time step  $t$  for prompt  $p$ . When the generative trajectory fails to regulate these tensions, hallucinations emerge—not as random outliers, but as structured projection shifts resulting from excessive load or directional misbalance in cognitive constraints.

We identify two key indicators of tension-induced risk:

$$|\vec{\tau}|_2 > \theta(p) \quad \text{or} \quad \text{Var}(\vec{\tau}) > \delta \quad (5)$$

Here,  $|\vec{\tau}|_2$  measures the total alignment stress across all axes, and  $\text{Var}(\vec{\tau})$  reflects tension anisotropy. Either elevated cumulative tension or pronounced directional skew can independently destabilize the generation process. High overall tension (with low variance) signals task difficulty or overloaded alignment pressure, while high anisotropy (with lower magnitude) reveals selective misalignment along specific axes. In both cases, the generative trajectory is susceptible to drift into incongruent regions of  $\mathcal{T}^3$ , producing hallucinated outputs. We refer to this phenomenon as a **cognitive tension-induced trajectory deviation**.

#### 4.2 TRAJECTORY DRIFT FROM MISALIGNED TENSIONS.

To quantify how alignment tension imbalance translates into hallucinated outputs, we formalize the generative deviation as a **trajectory drift**  $\Delta \vec{t}$ —a directional shift in the trajectory caused by cumulative cognitive misregulation. Specifically, as the model progresses through denoising steps, unresolved tensions along SC, SA, and KG axes distort the latent dynamics, pushing the trajectory away from the prompt-aligned manifold  $\mathcal{M}_{\text{ideal}}$ .

To make this projection shift interpretable and tractable, we model it as a trajectory drift component induced by cumulative anisotropic tension. The additional force  $\Gamma(\vec{\tau}) \cdot n(z)$  represents a directional

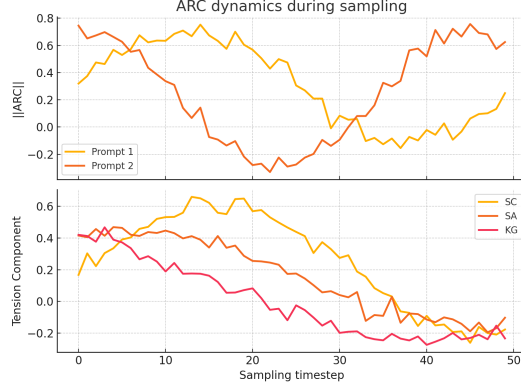


Figure 4: **ARC Dynamics.** (top) Total tension  $\|ARC\|$  across timesteps for two example prompts; (bottom) Component-wise trajectories showing tension concentration patterns that predict semantic vs. structural hallucinations.

deviation from the ideal trajectory, where  $\Gamma(\vec{\tau})$  is a learned mapping from the alignment risk vector  $\vec{\tau} = [\tau_{sc}, \tau_{sa}, \tau_{kg}]$  to a perturbation coefficient that scales with both the **magnitude** and **imbalance** of tension. A higher magnitude  $|\vec{\tau}|$  indicates elevated alignment stress, while larger variance among  $\tau_i$  components reveals tension anisotropy.

In this view, hallucinations are not caused by abrupt noise but by a **persistent, directionally biased shift** in the generative trajectory, where one or more tension components dominate and steer the diffusion process into biased latent regions outside the prompt-aligned manifold  $\mathcal{M}_{ideal}$ . We formalize this drift as:

$$\Delta \vec{t} = \Gamma(\vec{\tau}) \cdot n(z), \quad \text{where} \quad \Gamma(\vec{\tau}) = \lambda \cdot (|\vec{\tau}| + \beta \cdot \text{Var}(\vec{\tau})) \quad (6)$$

Here,  $\lambda$  and  $\beta$  are sensitivity coefficients controlling how total tension and tension imbalance contribute to the drift intensity. This formulation enables dynamic reasoning over hallucination risk during generation and sets the foundation for the trajectory-aware controller we describe next.

## 5 ALIGNMENT RISK CODE: MODELING HALLUCINATION TENSIONS IN T2I DIFFUSION

To quantitatively model the internal forces that drive projection shifts during image generation, we introduce the **Alignment Risk Code (ARC)**, a dynamic tension vector that encodes the instantaneous alignment pressures along key cognitive axes. This section first formalizes the generative space as a tri-orthogonal cognitive field, then defines how ARC captures both the magnitude and directionality of tension-induced deviations.

### 5.1 HALLUCINATION TRI-SPACE: SEMANTIC, STRUCTURAL, AND KNOWLEDGE TENSIONS

We conceptualize the diffusion process as a continuous trajectory  $z_0 \rightarrow z_1 \rightarrow \dots \rightarrow z_T$  in a high-dimensional latent space  $\mathcal{M}$ . Given a prompt  $p$ , this space implicitly encodes three orthogonal cognitive alignment subspaces:

$$\mathcal{M} = \mathcal{M}_{SC} \oplus \mathcal{M}_{SA} \oplus \mathcal{M}_{KG} \quad (7)$$

Let  $P_i : \mathcal{M} \rightarrow \mathcal{M}_i$  denote the projection operator onto subspace  $\mathcal{M}_i$  ( $i \in \{SC, SA, KG\}$ ). At each timestep  $t$ , the model’s latent state  $z_t$  is subject to corrective forces aimed at satisfying each alignment objective. We define the instantaneous cognitive tension along axis  $i$  as the norm of the alignment gradient:

$$\tau_i(p, t) = \|\nabla_{z_t} \mathcal{A}_i(z_t, p)\| \quad (8)$$



Here,  $\mathcal{A}_i(z_t, p)$  is a scalar potential function reflecting how well latent state  $z_t$  aligns with the  $i$ th cognitive goal. A large  $\tau_i$  implies strong restorative pressure in subspace  $\mathcal{M}_i$ .

Figure 3 visualizes this tension space. Ideal generation maintains low and balanced  $\tau_i$  values, preserving trajectory alignment with  $\mathcal{M}_{\text{ideal}}$ . However, when  $\vec{\tau}$  becomes both large in norm and skewed in distribution, the trajectory bends toward a biased submanifold, leading to hallucinations aligned with dominant tension directions.

## 5.2 ALIGNMENT RISK CODE: QUANTIFYING REAL-TIME TENSION DYNAMICS

We define the **Alignment Risk Code (ARC)** as a vector of instantaneous cognitive tensions at step  $t$ :

$$\vec{\tau}(p, t) = [\tau_{SC}(p, t), \tau_{SA}(p, t), \tau_{KG}(p, t)]^T \in \mathbb{R}^3 \quad (9)$$

The ARC vector provides a real-time, physically grounded representation of the internal alignment state of the model. From this vector, we derive interpretable measures:

- **Tension magnitude:**  $\|\vec{\tau}(p, t)\|_2$ , indicating the overall alignment stress.
- **Tension imbalance:**  $\text{Var}(\vec{\tau}(p, t))$ , measuring the anisotropy of tension distribution.
- **Tension skew:**  $\text{Softmax}(\vec{\tau})$ , yielding a probability-like attribution of hallucination directionality.

Tracking  $\vec{\tau}$  across diffusion steps reveals dynamic shifts in alignment priorities and exposes emerging risks of hallucination. As illustrated in Figure 4, certain prompts induce consistent dominance in specific  $\tau_i$  components, leading to failure modes that are not random but axis-dependent.

The ARC formulation thus transforms latent alignment pressures into a structured, actionable representation. In the next section, we leverage this vector to develop a control mechanism that dynamically mitigates hallucinations by counteracting emerging tensions in real time, without requiring retraining of the base diffusion model.

## 6 TENSIONMODULATOR: ARC-GUIDED HALLUCINATION CONTROL MECHANISM

While the Alignment Risk Code (ARC) provides a real-time representation of cognitive tension during generation, it also enables a closed-loop correction framework. We introduce **TensionModulator (TM-ARC)**, a lightweight, modular controller that applies dynamic perturbations to the generative trajectory in response to instantaneous tension signals. TM-ARC transforms ARC from a descriptive diagnostic vector into an actionable feedback mechanism, actively preventing directional drift toward the ideal manifold  $\mathcal{M}_{\text{ideal}}$ .

### 6.1 MOTIVATION FOR TENSION-GUIDED FEEDBACK CONTROL

Standard diffusion models perform open-loop sampling with no mechanism to monitor or correct internal misalignments. When tension imbalances accumulate, whether due to prompt ambiguity or model inductive bias, they steer the latent trajectory away from the prompt-aligned semantic manifold  $\mathcal{M}_{\text{ideal}}$ . Without real-time regulation, such misalignments manifest as hallucinations in the final image. By contrast, TM-ARC continuously senses the ARC vector  $\vec{\tau}(p, t)$  and injects targeted restorative signals that realign the generation path. The objective is not to eliminate variability, but to suppress excursions into tension-saturated regions that result in semantically, structurally, or factually implausible outputs.

### 6.2 MODULAR DECOMPOSITION BY TENSION AXES

TM-ARC decomposes into three orthogonal sub-controllers, each aligned with a distinct cognitive alignment dimension:



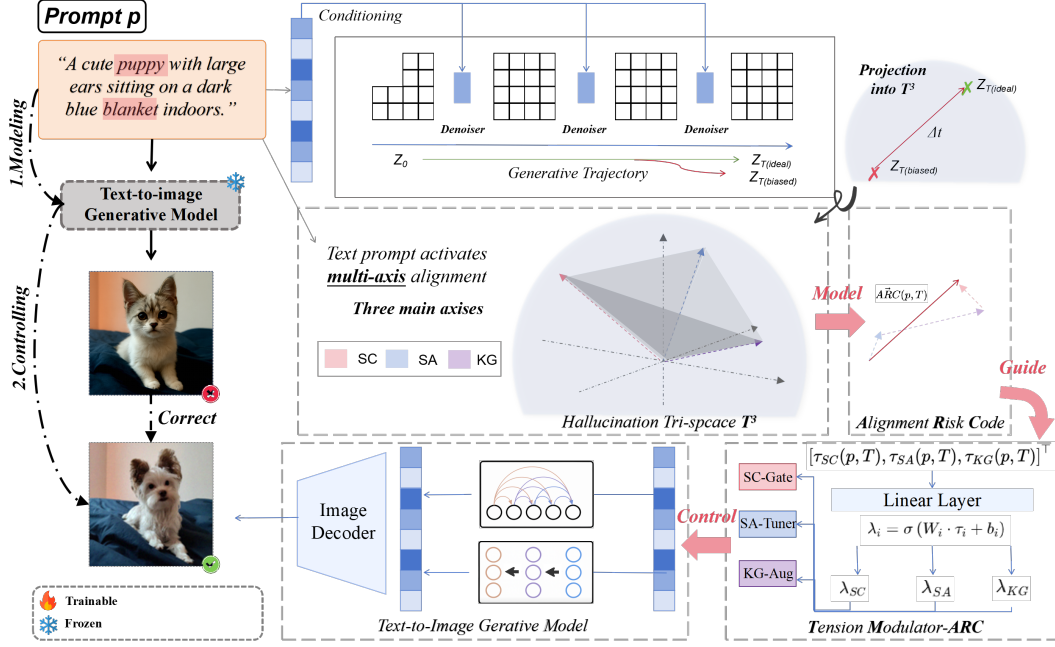


Figure 5: **Overview of hallucination modeling and ARC-guided control in T2I generation.** Given a prompt  $p$ , the T2I model undergoes iterative denoising, where semantic (SC), structural (SA), and knowledge (KG) alignment tensions dynamically evolve within the Hallucination Tri-Space  $\mathcal{T}^3$ . Misregulated tension leads to a trajectory drift  $\Delta t$  from the ideal generative path. The Alignment Risk Code (ARC) encodes real-time multi-axial tension and guides the Tension Modulator (TM-ARC) to inject adaptive controls via SC-Gate, SA-Tuner, and KG-Aug modules for hallucination mitigation.

- **SC-Gate** ( $F_{SC}$ ): Reactivates attention on prompt-critical entities when semantic tension  $\tau_{SC}$  intensifies, counteracting semantic drift through modulation of decoder focus.
- **SA-Tuner** ( $F_{SA}$ ): Refines latent spatial encodings when structural tension  $\tau_{SA}$  rises, preserving object placement and spatial logic via positional re-weighting.
- **KG-Augment** ( $F_{KG}$ ): Injects auxiliary factual priors or semantic anchors when knowledge tension  $\tau_{KG}$  surges, reinforcing commonsense consistency. It operates in two complementary modes:
  - *Static injection*: KG-related prompt embeddings are prepended to the text encoder input to provide prior knowledge.
  - *Dynamic modulation*: Cross-attention layers are reweighted based on  $\tau_{KG}$  to emphasize or suppress contextually relevant facts during generation.

Each submodule operates as a soft perturbation function over the latent state  $z_t$ , guided solely by the corresponding ARC component. The modular structure ensures that each intervention remains interpretable and independently tunable.

### 6.3 ARC-DRIVEN FEEDBACK DYNAMICS

At each generation step  $t$ , TM-ARC modifies the latent code according to a gated composite function:

$$z_t \leftarrow z_t + \lambda(\vec{\tau}(p, t)) \cdot \sum_{i \in \{SC, SA, KG\}} F_i(z_t, \tau_i(p, t)) \quad (10)$$

- $\lambda(\vec{\tau}) = \sigma(\|\vec{\tau}\|_2)$  is a tension-adaptive scaling function that increases modulation strength with overall tension magnitude;

- $F_i(z_t, \tau_i)$  denotes the  $i$ -th correction operator, each modulated by its corresponding tension signal;
- Each  $F_i$  is differentiable and temporally localized, ensuring responsiveness without introducing global disruption.

This formulation allows TM-ARC to function analogously to a physical damping system: minimal corrections under low tension, and strong directional feedback when misalignment intensifies.

#### 6.4 INTEGRATION AND GENERALIZATION

TM-ARC is designed as a plug-and-play augmentation for pretrained diffusion models. It operates entirely in the latent space and requires no additional supervision, training, or architecture modification. The modular design ensures compatibility across model backbones and preserves zero-shot generalizability. Because its intervention is conditioned solely on ARC: a model-internal, prompt-dependent signal, TM-ARC generalizes across unseen prompts and domains, as long as alignment tension can be monitored.

By continuously sensing the evolving semantic, structural, and knowledge alignment tensions during generation, TM-ARC actively intervenes to guide the generative path back toward a cognitively balanced state. Thus, TM-ARC enables the first tension-aware feedback mechanism for hallucination mitigation in T2I diffusion, grounded in cognitive alignment dynamics rather than post hoc filtering or static constraints.

### 7 EXPERIMENTS

We conduct comprehensive experiments to evaluate both the representational capacity of the proposed **Alignment Risk Code (ARC)** and the hallucination mitigation performance of the **Tension-Modulator (TM-ARC)** controller. Our analysis focuses on four key questions: **(i)** Can ARC capture structured hallucination patterns in a low-dimensional and interpretable manner? **(ii)** Does modeling multi-axis tension provide tangible benefits over lower-dimensional baselines? **(iii)** Can ARC enable prompt-aware, real-time controllability during generation? **(iv)** Does the TM-ARC module scale to diverse diffusion backbones and benchmarks while improving semantic alignment and perceptual quality? The following subsections progressively address these questions through quantitative metrics, visualization analyses, and large-scale benchmark studies.

#### 7.1 3D ARC YIELDS THE MOST EXPRESSIVE AND SEPARABLE REPRESENTATION

We first evaluate ARC’s ability to capture hallucination-specific alignment tensions in an interpretable and discriminative manner. As shown in Table 2, ARC’s full 3D formulation, spanning semantic coherence, structural alignment, and knowledge grounding, achieves a classification accuracy of 91.6% and a silhouette score of 0.63. In contrast, collapsing ARC to 2D or 1D results in significant performance drops, indicating that hallucination patterns cannot be adequately captured by any subset of axes alone. This supports our hypothesis that hallucinations are inherently multi-axial, requiring complete cognitive tension modeling.

#### 7.2 AXIS-DOMINANT TENSION EXPLAINS HALLUCINATION FAILURES AND GUIDES TARGETED CORRECTION

Building on ARC’s representational capacity, we visualize hallucination decomposition across real prompts in Figure 6. Each example pair: faithful vs. hallucinated image, is accompanied by its ARC radar plot. Across diverse failure modes, hallucinations consistently align with specific tension spikes: semantic drift (e.g., “puppy”  $\rightarrow$  “cat”) manifests as elevated  $\tau_{SC}$ ; structural mismatch (e.g., *object placement errors*) correlates with  $\tau_{SA}$ ; factual grounding issues (e.g., *hallucinated “AI conference”*) are reflected in  $\tau_{KG}$ . Notably, our controller reduces the dominant spike while preserving balanced axes, showing that ARC is not only descriptive but also actionable.

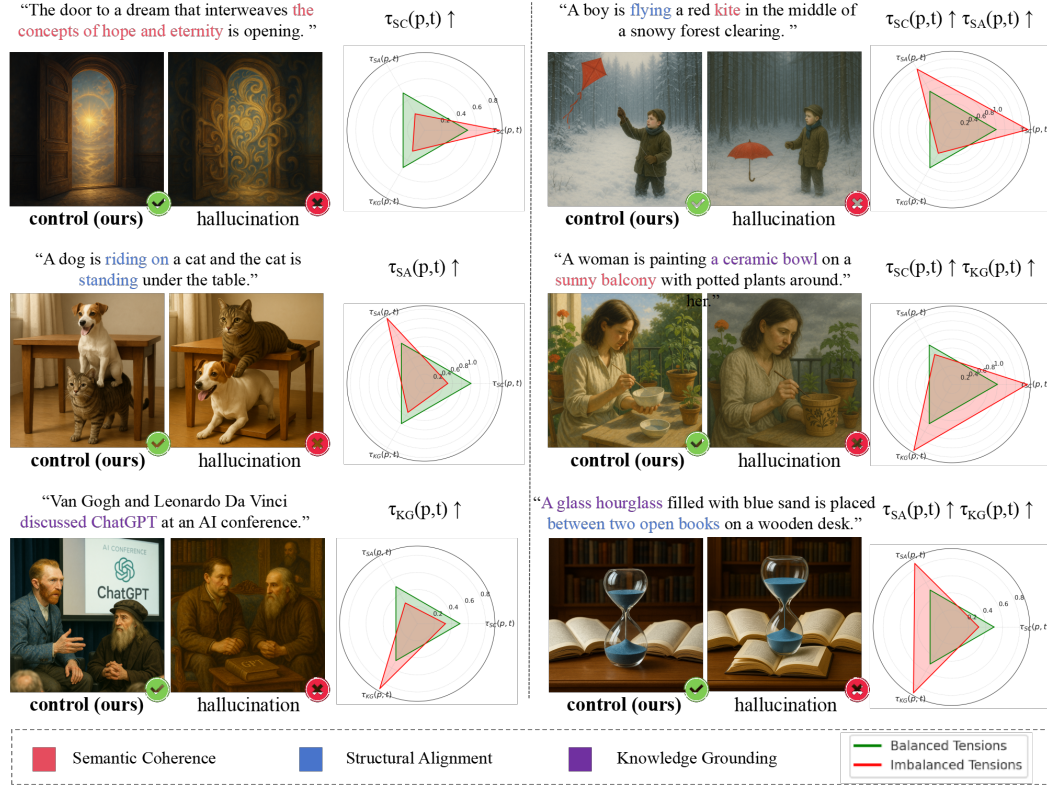


Figure 6: **Hallucination decomposition case studies.** Each example shows (from left to right): the original prompt fragment (highlighted in color), a correct generation (✓), a hallucinated output (✗), and its corresponding ARC radar plot. Green shaded triangles denote balanced alignment tension; red outlines show elevated tension and skew. Examples are categorized by dominant hallucination axis: semantic (blue), structural (red), and knowledge grounding (purple). ARC vectors reveal that hallucinations consistently align with dominant tension components, validating our modeling assumptions.

Table 2: Dimensionality ablation results on ARC representation.

ARC Dimension	Classification Accuracy	Silhouette Score
1D (best axis only)	78.2%	0.42
2D (any two axes)	86.7%	0.52
3D (full ARC)	<b>91.6%</b>	<b>0.63</b>

### 7.3 PROMPT-LEVEL ARC MODULATION SUBSTANTIALLY BOOSTS FAITHFULNESS

We next validate ARC’s role in enabling controllable generation. Table 3 shows that after TM-ARC modulation, ‘Flying Elephant’ and ‘Red Triangle’, both high-tension prompts, achieve +14.3 and +9.7 gains in faithfulness, respectively. The ARC vectors before and after intervention illustrate how the controller selectively attenuates risk-prone components. This demonstrates that ARC serves as a lightweight alignment monitor, enabling real-time axis-specific modulation during generation without retraining.

### 7.4 ARC GENERALIZES ACROSS BACKBONES AND OUTPERFORMS STRONG BASELINES

Finally, we benchmark ARC+TM-ARC on DrawBench and Pick-a-Pic across four diffusion models (Stable Diffusion XL (SDXL) Podell et al. (2023), SD1.5 Rombach et al. (2022), PixArt-sigma Chen et al. (2024), and Hunyuan-DiT Tencent AI Lab (2024)). As summarized in Table 4, our method

Table 3: ARC modulation and controllability performance.

Prompt	ARC (Before)	ARC (After)	Faith $\uparrow$
Flying Elephant	[0.92, 0.31, 0.41]	[0.48, 0.30, 0.35]	+14.3
Red Triangle	[0.33, 0.88, 0.27]	[0.29, 0.43, 0.24]	+9.7

Table 4: **Benchmark results on DrawBench and Pick-a-Pic.** Best results are **bolded**; second-best are underlined. Metrics: CLIPScore ( $\uparrow$ ), PickScore ( $\uparrow$ ), ImageReward (IR $\uparrow$ ), FID ( $\downarrow$ ).

Method	CLIP Score $\uparrow$	Pick Score $\uparrow$	IR $\uparrow$	FID $\downarrow$	CLIP Score $\uparrow$	Pick Score $\uparrow$	IR $\uparrow$	FID $\downarrow$
<i>DrawBench – SDXL</i>					<i>DrawBench – SD1.5</i>			
Vanilla	28.3	20.9	0.77	47.5	28.7	21.7	0.86	20.0
Prompt-to-Prompt	27.4	20.8	0.70	<u>27.0</u>	27.5	20.4	0.59	54.0
Attend-and-Excite	28.4	20.6	0.68	47.0	<b>29.9</b>	22.5	0.58	<u>26.5</u>
Zigzag Diff	<u>28.9</u>	21.1	<b>0.89</b>	52.0	27.4	<b>22.6</b>	<u>0.79</u>	42.5
<b>ARC (Ours)</b>	<b>29.3</b>	<b>21.6</b>	0.85	<b>20.0</b>	<u>28.7</u>	21.1	<b>0.89</b>	<b>20.0</b>
<i>DrawBench – PixArt-sigma</i>					<i>DrawBench – Hunyuan-DiT</i>			
Vanilla	29.2	20.9	0.63	39.0	29.1	21.7	0.80	57.0
Prompt-to-Prompt	27.6	20.6	0.77	58.5	28.5	20.0	<b>0.83</b>	33.0
Attend-and-Excite	27.3	<u>21.5</u>	0.71	30.5	<b>29.5</b>	20.0	<u>0.83</u>	54.0
Zigzag Diff	<u>29.1</u>	<b>21.6</b>	0.75	<u>24.6</u>	28.9	20.2	<b>0.83</b>	<u>49.5</u>
<b>ARC (Ours)</b>	<b>29.3</b>	21.5	<b>0.79</b>	<b>19.8</b>	<u>29.4</u>	<b>22.6</b>	0.81	<b>18.2</b>
<i>Pick-a-Pic – SDXL</i>					<i>Pick-a-Pic – SD1.5</i>			
Vanilla	29.4	21.0	0.71	41.5	28.8	21.9	0.72	68.0
Prompt-to-Prompt	27.4	21.6	0.70	34.5	<b>29.9</b>	21.5	0.58	47.0
Attend-and-Excite	28.3	<b>22.6</b>	0.76	36.5	28.8	<b>22.6</b>	0.72	33.5
Zigzag Diff	<u>29.1</u>	21.8	<u>0.86</u>	<b>20.5</b>	28.2	<u>22.5</u>	<u>0.79</u>	<u>29.5</u>
<b>ARC (Ours)</b>	<b>29.4</b>	22.0	<b>0.90</b>	<u>21.5</u>	<u>29.1</u>	22.4	<b>0.83</b>	<b>19.8</b>
<i>Pick-a-Pic – PixArt-sigma</i>					<i>Pick-a-Pic – Hunyuan-DiT</i>			
Vanilla	27.9	22.5	0.68	29.0	27.8	22.9	0.78	27.0
Prompt-to-Prompt	29.8	21.5	0.57	32.5	27.5	21.7	0.82	35.5
Attend-and-Excite	<b>29.8</b>	20.8	0.59	50.0	28.5	<b>22.9</b>	0.71	69.0
Zigzag Diff	28.6	22.1	<u>0.81</u>	<u>24.6</u>	27.2	21.5	0.69	<u>26.0</u>
<b>ARC (Ours)</b>	<u>29.7</u>	<b>22.5</b>	<b>0.83</b>	<b>17.7</b>	<b>29.1</b>	<u>22.7</u>	<b>0.83</b>	<b>18.8</b>

consistently surpasses strong baselines, including Prompt-to-Prompt Hertz et al. (2022), Attend-and-Excite Chefer et al. (2023), and Zigzag Diffusion Sampling Bai et al. (2024), on all major metrics: CLIPScore Hessel et al. (2021), PickScore Kirstain et al. (2023), ImageReward Xu et al. (2023), and FID Heusel et al. (2017). In particular, ARC delivers the best PickScore in 6 out of 8 settings and achieves lowest FID in 7 out of 8, confirming that our tension-driven control translates into higher perceptual quality and semantic alignment across architectures and datasets.

## 8 CONCLUSION

We offer a cognitively grounded perspective on hallucination formation in T2I diffusion models, introducing the Hallucination Tri-Space to model tension imbalances across semantic coherence, structural alignment, and knowledge grounding. This framing reveals hallucinations as projection shifts driven by alignment conflicts rather than random noise. To quantify these tensions, we propose the Alignment Risk Code (ARC), a dynamic vector that monitors alignment pressures throughout generation. On top of ARC, we develop TensionModulator (TM-ARC), a lightweight controller that adaptively regulates generation in real-time to preempt hallucinations without retraining. Extensive experiments validate the effectiveness, controllability, and generalization of our framework across diverse hallucination scenarios and model backbones. We hope this tension-centered mod-

eling framework offers a step forward towards interpretable, controllable, and safer generative systems.

## REFERENCES

- Lichen Bai, Shitong Shao, Zikai Zhou, Zipeng Qi, Zhiqiang Xu, Haoyi Xiong, and Zeke Xie. Zigzag Diffusion Sampling: Diffusion Models Can Self-Improve via Self-Reflection. *arXiv preprint arXiv:2412.10891*, 2024.
- Hyojin Chang, Menglin Li, Jisu Park, and Youngjoon Kim. Catastrophic neglect in text-to-image generation: Diagnosing and mitigating object hallucinations in diffusion models. In *Proceedings of the IEEE/CVF Conference on Computer Vision and Pattern Recognition (CVPR)*, 2024.
- Hila Chefer, Yuval Alaluf, Yael Vinker, Lior Wolf, and Daniel Cohen-Or. Attend-and-Excite: Attention-Based Semantic Guidance for Text-to-Image Diffusion Models. *arXiv preprint arXiv:2301.13826*, 2023.
- Yu Chen, Shiyang Li, Zhengyuan Yang, Jianshu Chen, and Nan Duan. Unified Hallucination Detection for Multimodal Large Language Models. In *Proceedings of the 62nd Annual Meeting of the Association for Computational Linguistics (ACL-2024)*, pp. 3195–3210, Bangkok, Thailand, 2024. Association for Computational Linguistics.
- Amir Hertz, Ron Mokady, Jay Tenenbaum, Kfir Aberman, Yael Pritch, and Daniel Cohen-Or. Prompt-to-Prompt Image Editing with Cross-Attention Control. In *CVPR*, 2022. *arXiv preprint arXiv:2208.01626*.
- Jack Hessel, Ari Holtzman, Maxwell Forbes, Ronan Le Bras, and Yejin Choi. CLIPScore: A Reference-free Evaluation Metric for Image Captioning. *arXiv preprint arXiv:2104.08718*, 2021.
- Martin Heusel, Hubert Ramsauer, Thomas Unterthiner, Bernhard Nessler, and Sepp Hochreiter. GANs Trained by a Two Time-Scale Update Rule Converge to a Local Nash Equilibrium. *Advances in Neural Information Processing Systems*, 30, 2017.
- Dongzhi Jiang, Guanglu Song, Xiaoshi Wu, Renrui Zhang, Dazhong Shen, Zhuofan Zong, Yu Liu, and Hongsheng Li. CoMat: Aligning Text-to-Image Diffusion Model with Image-to-Text Concept Matching. In *NeurIPS 2024 Poster*, 2024.
- Emily Johnson and Noah Wilson. Hierarchical Vision-Language Alignment for Text-to-Image Generation via Diffusion Models (VLAD). *arXiv preprint arXiv:2501.00917*, 2025.
- Yuval Kirstain, Adam Polyak, Uriel Singer, Shahbuland Matiana, Joe Penna, and Omer Levy. Pick-a-Pic: An Open Dataset of User Preferences for Text-to-Image Generation. In *NeurIPS 2023*, 2023.
- Jaa-Yeon Lee, Byunghee Cha, Jeongsol Kim, and Jong Chul Ye. Aligning Text to Image in Diffusion Models is Easier Than You Think (SoftREPA). *arXiv preprint arXiv:2503.08250*, 2025.
- Mingcheng Li, Xiaolu Hou, Ziyang Liu, Dingkan Yang, Ziyun Qian, Jiawei Chen, Jinjie Wei, Yue Jiang, Qingyao Xu, and Lihua Zhang. MCCD: Multi-Agent Collaboration-based Compositional Diffusion for Complex Text-to-Image Generation. In *CVPR 2025*, 2025.
- Yuna Lim and Honglak Shim. Retrieval-augmented diffusion: Mitigating hallucination in text-to-image generation via knowledge grounding. In *Proceedings of the AAAI Conference on Artificial Intelligence (AAAI)*, 2024.
- Rui Lu, Runzhe Wang, Kaifeng Lyu, Xitai Jiang, Gao Huang, and Mengdi Wang. Towards Understanding Text Hallucination of Diffusion Models via Analyzing Generation Patterns. *arXiv preprint arXiv:2503.03595*, 2025.
- Zheqi Lv, Junhao Chen, Qi Tian, Keting Yin, Shengyu Zhang, and Fei Wu. Multimodal LLM-Guided Semantic Correction in Text-to-Image Diffusion. *arXiv preprint arXiv:2505.20053*, 2025.

- Dustin Podell, Zion English, Kyle Lacey, Andreas Blattmann, Tim Dockhorn, Jonas Müller, Joe Penna, and Robin Rombach. SDXL: Improving Latent Diffusion Models for High-Resolution Image Synthesis. *arXiv preprint arXiv:2307.01952*, 2023.
- Robin Rombach, Andreas Blattmann, Dominik Lorenz, Patrick Esser, and Björn Ommer. High-Resolution Image Synthesis with Latent Diffusion Models. In *CVPR*, 2022.
- Tencent AI Lab. Hunyuan-DiT: A Powerful Multi-Resolution Diffusion Transformer for Bilingual Text-to-Image Generation. <https://github.com/Tencent/HunyuanDiT>, 2024.
- Luozhou Wang, Guibao Shen, Wenhao Ge, Guangyong Chen, Yijun Li, and Ying-cong Chen. Text-Anchored Score Composition: Tackling Condition Misalignment in Text-to-Image Diffusion Models. *arXiv preprint arXiv:2306.14408*, 2023.
- Yihang Wu, Xiao Cao, Kaixin Li, Zitan Chen, Haonan Wang, Lei Meng, and Zhiyong Huang. Towards Better Text-to-Image Generation Alignment via Attention Modulation. *arXiv preprint arXiv:2404.13899*, 2024.
- Jiazheng Xu, Xiao Liu, Yuchen Wu, Yuxuan Tong, Qinkai Li, Ming Ding, Jie Tang, and Yuxiao Dong. ImageReward: Learning and Evaluating Human Preferences for Text-to-Image Generation. *NeurIPS 2023*, 2023.
- Wei Zhang, Tianhao Zhou, Zhenyu Huang, and Xuehai Li. Attention refocusing for faithful text-to-image generation. In *Proceedings of the IEEE/CVF Conference on Computer Vision and Pattern Recognition (CVPR)*, 2024.
- Qin Zhou, Zhiyang Zhang, Jinglong Wang, Xiaobin Li, Jing Zhang, Qian Yu, Lu Sheng, and Dong Xu. ELBO-T2IAlign: A Generic ELBO-Based Method for Calibrating Pixel-level Text-Image Alignment in Diffusion Models. *arXiv preprint arXiv:2506.09740*, 2025.